

Fluctuation Enhancement and Reduction in Sheared Polymer Solutions

Denis Wirtz

Chemical Engineering Department, The Johns Hopkins University,
Baltimore, Maryland 21218

Received April 25, 1994*

ABSTRACT: Using time-resolved small-angle light scattering, we present the first experimental evidence that a semidilute polymer solution successively subjected to a high-strain-rate shear flow followed by a low-strain-rate shear flow displays concentration fluctuation enhancement and fluctuation reduction (Maxwell effect), respectively. During the Maxwell fluctuation reduction, the flow-induced intermediate scattering peaks present in the structure factor at high strain rates are eliminated and the scattering patterns rotate toward a direction at 90° with the flow direction. The Maxwell rotation and stretching of the shear-enhanced fluctuations and the corresponding pattern orientation angle are satisfactorily described by the so-called Maxwell construction applied to the Helfand–Fredrickson structure factor of the shear-enhanced fluctuations.

1. Introduction

This paper presents the first experimental evidence of successive fluctuation enhancement and reduction in the dynamics of sheared polymer solutions near the critical point. The enhancement of concentration fluctuations by an external flow field effect in polymeric systems has recently received much attention from both theoretical^{1–3} and experimental^{4–7} viewpoints. Helfand and Fredrickson (HF) were the first authors to unravel the mechanism of fluctuation enhancement. This HF effect consists of the dramatic flow-induced *increase* of the concentration fluctuations due to an effective coupling between the polymeric shear stress and the concentration fields via concentration-dependent transport coefficients.¹ This dynamical coupling is at the origin of the phenomenon of flow-induced phase separation of semidilute polymer solutions in simple shear^{4–7} and extensional flows.⁷ More generally, this effect can be present when the coupling is strong enough between an external shear flow and the long-lived internal degrees of freedom of a fluid system. Flow-induced fluctuation enhancement is observed in lyotropic liquid crystals, swollen gels, colloidal suspensions, and membranes under shear.⁹

The Maxwell effect, instead, describes the *reduction* of the concentration fluctuations in the presence of a shear flow and their simultaneous alignment toward the flow direction. In Figure 1 is depicted a schematic of the Maxwell stretching and clockwise rotation of the fluctuation clusters in the flow direction in the real space and the corresponding stretching and counterclockwise rotation of the scattering patterns in the reciprocal space. The Maxwell effect can greatly affect the physical properties of a fluid. For instance, the phase transition of near-critical binary mixtures becomes second-order and the critical exponents recover their mean-field value.¹⁰ The Maxwell effect is observed in simple binary mixtures,¹⁰ ternary polymer solutions,¹¹ and polymer blends¹² in shear flows.

In the present paper, we demonstrate that a semidilute polymer solution successively subjected to a high-strain-rate and a low-strain-rate shear flow displays *both* Maxwell and HF behaviors. This result is unexpected because the two effects are antagonistic and exclude each other a priori.

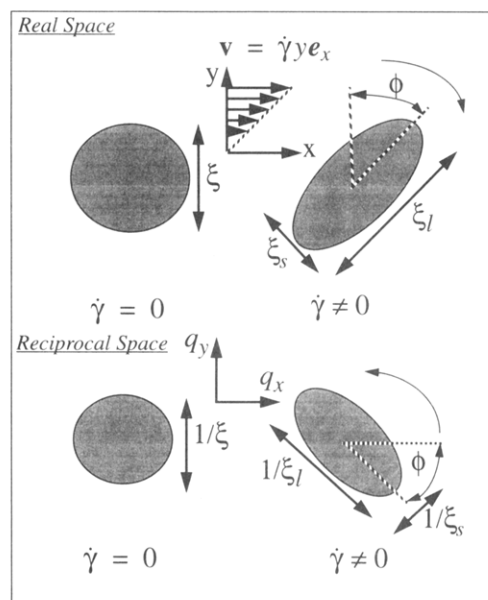


Figure 1. Maxwell rotation and stretching of a concentration fluctuation in a uniform shear flow, both in the real space and in the reciprocal Fourier space. In the real space, the initially isotropic fluctuation of average size ξ is anisotropically stretched and rotated in the flow direction, with new long and short correlation lengths ξ_l and ξ_s . The arrows indicate the sense of rotation of the fluctuations and their Fourier transform counterparts; the notations are defined in the text.

2. Experimental Section

In order to compare our findings to results previously published in the literature, the present polymer system is the widely used^{4–7} semidilute solution of polystyrene in dioctyl phthalate (PS/DOP). The molecular weight of the polymer is $M_w = 1\,850\,000$, with an index of polydispersity of $M_w/M_n = 1.06$ and a polymer concentration $c = 6$ wt % larger than the semidilute crossover concentration, c^* . This polymer solution is sheared in a Couette flow cell, maintained at a constant temperature T ($\pm 0.1^\circ$ deg), between the cloud point temperature T_c and the θ temperature of the solution, $T_c = 11^\circ\text{C} < T = 16^\circ\text{C} < \theta = 22^\circ\text{C}$. The gap width between the two concentric cylinders of the cell is 0.36 cm; the light path length through the sample is 1 cm. The dynamics of fluctuation orientation are monitored by time-resolved small-angle light scattering (SALS) in the plane of the flow and shear directions, normal to the incident light of a He–Ne laser ($\lambda = 632.8$ nm). Images are acquired via a CCD array camera and a framegrabber at a frame rate of up to three images per second.

* Abstract published in *Advance ACS Abstracts*, September 1, 1994.

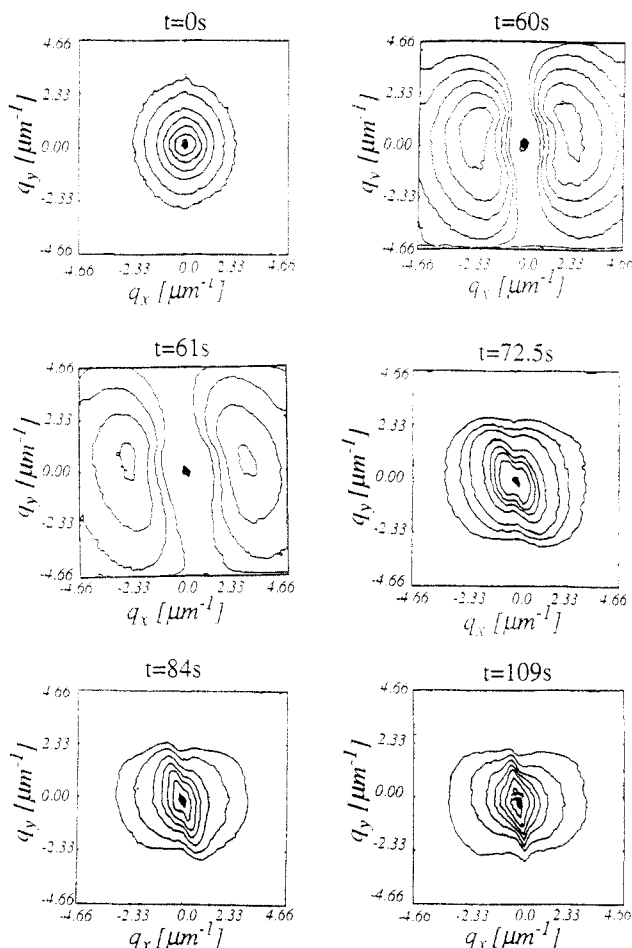


Figure 2. Evolution of SALS patterns produced by a semidilute PS/DOP solution subjected to a shear flow with two successive shear rates. (1) Quiescent state in the absence of flow. (2) Steady state HF scattering pattern after 60 s; $\dot{\gamma} = 1.8 \text{ s}^{-1}$. (3) Relaxation of the scattering patterns after 61 s. (4) Onset of the Maxwell effect, $\dot{\gamma} = 0.02 \text{ s}^{-1}$, $t = 72.5 \text{ s}$. (5) $t = 84 \text{ s}$. (6) Steady state, $t = 109 \text{ s}$. The system is a 6 wt % PS/DOP solution at 16°C .

Frames are then analyzed using the software SALS.^{4,8} Further experimental details on the cell geometry, the SALS technique, and the image acquisition procedure are given in refs 4 and 13.

3. Results and Discussion

Effective coupling between the concentration fluctuations and an external flow field is expected when the flow time scale $\dot{\gamma}^{-1}$ is of the same magnitude as the relevant time scale of the polymer solution τ : $De = \dot{\gamma}\tau \geq 1$. Here, $\dot{\gamma}$ is the uniform shear rate produced by the Couette flow cell. The rheological relaxation time was previously measured⁴ for our polymer solution and is equal to $\tau \approx 0.995 \text{ s}$ at $T = 16^\circ\text{C}$. The experimental protocol includes a strong flow ($De \geq 1$) and a weak flow ($De \ll 1$), successively. Each experiment is composed of three steps. First, the PS/DOP solution is sheared at a high deformation rate ($De \geq 1$) until steady state is reached. In this case, the major axis of the light scattering patterns is oriented at an angle ϕ_0 with the flow direction, decreasing from approximately $\phi_0 \sim 30^\circ$ to $\phi_0 \sim -15^\circ$ with shear rates increasing from $De = 0.2$ to $De = 2.5$. Second, the flow field is turned off for a short time period on the order of τ . Third, the resulting (slowly decaying) enhanced concentration fluctuations are sheared at very low shear rates ($De \ll 1$) to avoid the HF effect. This last step induces the ensemble rotation and stretching of the fluctuation clusters toward the flow direction.

Figure 2 displays a typical set of the resulting SALS patterns taken at different relevant moments of the

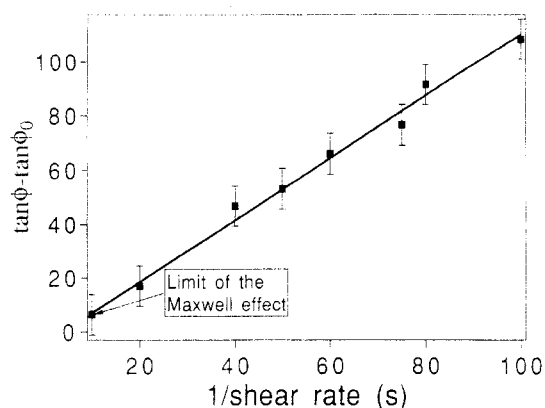


Figure 3. Measured angle ϕ of the major axis of the scattering patterns with respect to the flow direction as a function of inverse shear rate $\dot{\gamma}^{-1}$. The line is the best linear fit; its slope yields a relaxation time $\tau \approx 0.87 \text{ s}$. Same polymer solution as in Figure 2.

experiment. Scattering patterns correspond to iso-intensity contours of the light scattered by the sheared polymer solution. The first two pictures in Figure 2 respectively correspond to the isotropic, quiescent state in the absence of flow and the steady state scattering pattern after the solution is sheared for 2 min ($De = 1.8$). In this case, the pattern displays enhanced scattering at an angle close to the flow direction. Helfand and Fredrickson (HF)¹ demonstrated that the mechanism responsible for this fluctuation enhancement is an effective coupling between the fluctuating viscoelastic stress and the polymer concentration fluctuation fields. The lifetime of the concentration fluctuations is dramatically (and anisotropically) increased due to flow-induced enhanced elastic stress. Further, Figures 2 and 3 show the onset of two flow-induced broad scattering peaks located at an intermediate wavelength, $\lambda_{\text{peak}} = 2\pi/q_{\text{peak}} = 1.78 \mu\text{m}$. We recently demonstrated¹⁴ that these scattering peaks result from combined effects of HF fluctuation enhancement and advection of the fluctuations.¹⁴ In addition, recent SALS experiments¹⁴ showed that the steady-state distance of the peaks from the origin of the reciprocal space scales like $\dot{\gamma}^{1/2}$, at low shear rates.

The third frame in Figure 2 displays the scattering pattern just before the solution is resheared, after the flow has been turned off for 1 s. The scattering intensity is decreased in this case, but a large light scattering overshoot generally occurs for shear rates $De \geq 4$ at $T = 16^\circ\text{C}$,⁴ due to elastic recoil of the polymer. In addition, Dixon *et al.*⁷ have recently demonstrated that, upon cessation of flow, the slow mode of relaxation is naturally selected, whereas both slow and fast modes are present in the quiescent state (as measured by dynamic light scattering, for example).

The last three frames describe two coexisting effects after inception of a low-strain-rate shear flow ($De = 0.05$). First, the two intermediate scattering peaks are eliminated.^{7,14,15} As a result, the maximum intensity occurs at the origin of the Fourier space. This unexpected effect is seen by comparing Figures 2b,d. Second, the scattering is reduced in the direction parallel to the flow direction and reduced at large q values, while the scattering light remains significant in the direction normal to the flow. The patterns are elongated and oriented in the direction normal to the flow field in the small- q region. Such anisotropic scattering patterns are a signature of stretched fluctuation clusters aligning toward the flow direction. The resulting fluctuation deformation increases the cost of the elastic energy of creating a fluctuation, and therefore

anisotropically suppresses fluctuations in shear. Note that these fluctuation clusters have no sharp boundaries; hence, they cannot be considered as droplets with a finite surface tension.⁹ Otherwise, beyond a certain strain, the stretched fluctuation clusters would break into smaller droplets (Rayleigh instability). A quasi steady state is eventually reached, until the long-lived, pretransitional fluctuations die off, and the Maxwell effect re-emerges at large strains.

The measured scattering intensity is directly proportional to the structure factor, which is the Fourier transform of the equal-time correlation function. Therefore, further insight into the onset of the HF effect followed by the Maxwell effect could be gained by full analysis of an equation of motion of the structure factor in the presence of two successive flow analysis of an equation of motion of the structure factor in the presence of two successive flow fields of decreasing shear rates.^{1,2,9} However, in the present case, the Maxwell rotation of the large fluctuations in a simple shear $\nu = \dot{\gamma} y e_x$ can approximately be described by the so-called Maxwell construction:⁹

$$S(\mathbf{q}, t) \cong S_0(\mathbf{q})[1 - \exp(-2t/\tau_0(\mathbf{q}))] + S_{HF}(\mathbf{q}) \exp(-2t/\tau_0(\mathbf{q}))|_{\mathbf{q} = \mathbf{q} + \dot{\gamma} \tau(\mathbf{q}) \mathbf{q}_y e_y} \quad (1)$$

where S_0 is the equilibrium Ornstein-Zernike structure factor with $\tau_0(q) = (\eta/k_B T) S_0(q)$; S_{HF} is the steady-state, nonequilibrium HF¹ structure factor in the presence of a uniform shear flow, $S_{HF}^{-1}(\mathbf{q}) \cong \partial^2 f / \partial \varphi + q^2 \xi^2 - (\partial \tau_{ij} / \partial \varphi) \cdot \mathbf{q}_i \mathbf{q}_j / q^2$; and $\tau(\mathbf{q}) = (\eta/k_B T) S_{HF}(\mathbf{q})$ is the anisotropically enhanced lifetime of concentration fluctuations. Of course, this simplification does not hold in the high-shear-rate regime, especially in the low- q region,¹⁴ where advection effects dominate the transport of the concentration fluctuations. Here, $\partial \tau / \partial \varphi$ is the concentration derivative of the fluctuating polymer stress tensor τ , f is the Flory-Huggins free energy density, φ is the polymer volume fraction, q_i are the Cartesian coordinates of the scattering vector \mathbf{q} , k_B is the Boltzmann constant, η is the solution viscosity, and ξ is the quiescent correlation length of the fluctuation. Equation 1 represents the rotation of the initial HF structure factor toward the axis normal to the flow. The corresponding quasi steady state angle, ϕ , of the scattering patterns with respect to the flow direction is given by $\tan 2\phi \cong 1/De$. The measured average angle of orientation of the scattering patterns is estimated by

$$\tan 2\phi = \frac{2\langle q_x q_y \rangle}{\langle q_x q_x \rangle - \langle q_y q_y \rangle} \quad (2)$$

where $\langle q_i q_j \rangle = \int d\mathbf{q} S(\mathbf{q}) q_i q_j / \int d\mathbf{q} S(\mathbf{q})$. The inverse of the slope of the linear fit gives a relaxation time $\tau \cong 0.87$ s, which compares favorably with previous rheological measurements⁴ for the same polymer/solvent system and at the same temperature distance from the coexistence curve. Figure 4 is a typical evolution of the angle of the scattering patterns using eq 2. The quiescent polymer solution is sheared to produce large fluctuations oriented at $\phi_0 \cong -8^\circ$. The final shear rate is smaller than the initial shear rate, with $De = 0.05 \ll 1$; therefore the scattering angle is decreased toward $\phi \cong -82^\circ$. Moreover, the rate at which the Maxwell steady-state scattering angle is reached increases with shear rate. As described below, the inverse effect is observed if the final shear rate is decreased, but with $De = O(1)$. Here, the measured scattering angle is increased.

It is important to note that if a low-shear-rate flow ($De \ll 1$) is applied first, followed by a strong shear flow, only

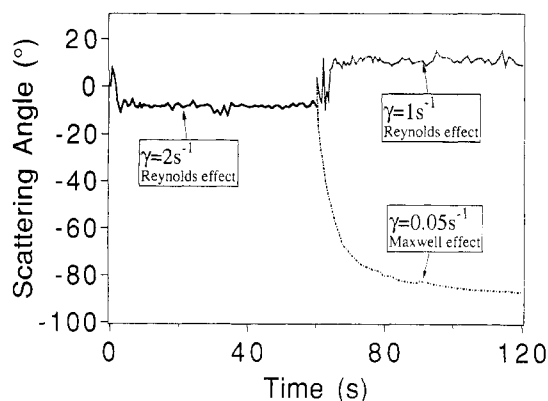


Figure 4. Typical evolution of the angle of the major axis of the scattering patterns with respect to the flow direction for an initial shear rate of 2 s^{-1} and two different final shear rates of 0.05 and 1 s^{-1} . These two different final shear rates induce the onset of the Maxwell effect or the HF effect, respectively. The flow is turned on at $t = 0$ s, turned off at $t = 50$ s, and turned on again at $t = 51$ s. Same polymer solution as in Figure 2.

the HF fluctuation enhancement mechanism is triggered. Several other interesting variations in the above experimental protocol are also possible. For example, if the final shear rate is smaller than, but of the same order of magnitude as ($De = O(1)$), the initial high shear rate, scattering grows in the new preferred direction according to the new symmetry dictated by the concentration-elastic stress coupling, with an increased average scattering angle, and without visible rotation of the patterns. As a result, in this case, no Maxwell rotation of the scattering patterns is observed. This general re-orientation of the scattering patterns can be seen in the upper curve of Figure 4. The scattering angle increases from $\phi_0 \cong -8^\circ$ to $\phi \cong 11.3^\circ$ when the shear rate is decreased from $De = 2$ to $De = 1$. On the contrary, if the final shear rate is larger than that of the initial part of the experimental protocol, then the HF effect completely dominates the pattern formation. The branching point corresponding to the critical final shear rate, where the scattering angle starts decreasing instead of increasing, is found to be $De \cong 0.2$. It is also important to note that the Maxwell rotation of the scattering structure factor only occurs at small deformation times; the Maxwell effect eventually vanishes, and the HF effect dominates at large strains. As a consequence, the Maxwell effect at long times is only obtained when the second flow is "weak" ($De \ll 1$).

Finally, if the direction of shearing is suddenly reversed (in the third step of the above experimental protocol), then scattering patterns rotate counterclockwise, as long as $De \ll 1$. Similarly, if the polymer solution is subjected to a small amplitude oscillatory shear flow, the resulting oscillatory motion of the resulting patterns is in phase with the shear in the large- q region (small fluctuations) and increasingly retards as the origin of the reciprocal space is approached (large fluctuations). Since the current image acquisition rate is limited to three images per second, this new effect of Maxwell rotation of the concentration fluctuations under oscillatory shear is left as a future extension of the present work.

Similar combined Maxwell and HF behaviors have been predicted⁹ for pretransitional lyotropic smectic A fluctuation clusters just above the nematic-smectic A transition point in simple shear. However, as pointed out by Bruinsma and Rabin,⁹ several important differences exist between the nematic-smectic A phase transition and the phase-separation point in binary fluids. In particular, in the present case of a binary fluid, the order parameter fluctuation is a conserved quantity.

4. Conclusion

We have shown that the large HF concentration fluctuations, generated by a strong shear flow, can be stretched and rotated (Maxwell effect) toward the flow direction by application of a weak shear. In addition, during the Maxwell rotation, the flow-induced scattering peaks in the structure factor are rapidly eliminated and transported toward the origin of the Fourier space. Using time-resolved SALS, the steady-state pattern orientation angle is computed, which confirms a Maxwell mechanism of stretching and alignment of the fluctuations in the flow direction. As an extension of the present work, the orientation of the large fluctuations produced by the HF effect could be monitored by other types of external fields including an electric field,¹³ an acoustic wave,¹⁶ or a magnetic field.¹⁷

Acknowledgment. I thank G. G. Fuller and the members of the rheo-optics group in the Chemical Engineering Department at Stanford University for their hospitality during my stay. In particular, I gratefully acknowledge valuable experimental help from J. Lai and D. E. Werner. Fruitful discussions with J. Harden are acknowledged. This research was partially funded through a postdoctoral fellowship from the "Human Capital and Mobility" program of the EU.

References and Notes

- (1) Helfand, E.; Fredrickson, G. H. *Phys. Rev. Lett.* **1989**, *62*, 2468.
- (2) Milner, S. T. *Phys. Rev. Lett.* **1991**, *66*, 1477. Milner, S. T. *Phys. Rev. E* **1994**, *48*, 3674.

- (3) Doi, M. In *Dynamics and Patterns in Complex Fluids*; Onuki, A., Kawasaki, K., Eds.; Springer Proceedings in Physics 52; Springer-Verlag: Heidelberg, Germany, 1990.
- (4) van Egmond, J. W.; Werner, D. E.; Fuller, G. G. *J. Chem. Phys.* **1992**, *96*, 7742.
- (5) (a) Hashimoto, H.; Takebe, T.; Suehiro, S. *J. Chem. Phys.* **1988**, *88*, 5874. (b) Moses, E.; Kume, T.; Hashimoto, T. *Phys. Rev. Lett.* **1994**, *72*, 2037.
- (6) Wu, X.-l.; Pine, D. J.; Dixon, P. K. *Phys. Rev. Lett.* **1991**, *62*, 2408.
- (7) Dixon, P. K.; Pine, D. J.; Wu, X.-l. *Phys. Rev. Lett.* **1992**, *66*, 2239.
- (8) van Egmond, J. W.; Fuller, G. G. *Macromolecules* **1994**, *26*, 7182.
- (9) (a) Bruinsma, R.; Safinya, C. R. *Phys. Rev. A* **1991**, *43*, 5377. (b) Bruinsma, R.; Rabin, Y. *Phys. Rev. A* **1992**, *45*, 994. (c) Bruinsma, R.; Y, Rabin, Y. *Phys. Rev. E* **1994**, *49*, 554.
- (10) (a) Onuki, A.; Kawasaki, K. *Ann. Phys.* **1979**, *121*, 456. (b) Onuki, A.; Kawasaki, K. *Phys. Lett. A* **1979**, *72*, 233. (c) Zalcser, G.; Bourgou, A.; Beysens, D. *Phys. Rev. A* **1983**, *28*, 440.
- (11) (a) Takebe, T.; Fujioka, K.; Hashimoto, T. *J. Chem. Phys.* **1990**, *88*, 5874. (b) Lai, J.; and Fuller, G. G. Submitted for publication to *J. Polym. Sci., Part B: Polym. Phys.*
- (12) Werner, D. E.; Franck, C. W.; Fuller, G. G. Unpublished results.
- (13) (a) Wirtz, D.; Berend, K.; Fuller, G. G. *Macromolecules* **1992**, *25*, 7234. (b) Wirtz, D.; Fuller, G. G. *Phys. Rev. Lett.* **1993**, *71*, 2236. (c) Wirtz, D.; Werner, D. E.; Fuller, G. G. *J. Chem. Phys.* **1994**, *101*, 1679.
- (14) Wirtz, D. Accepted for publication in *Phys. Rev. E*.
- (15) Upon the cessation of flow, the scattering angle generally decreases suddenly. ϕ_0 is the angle just before re-inception of the shear flow.
- (16) Onuki, A.; Oppenheim, I. *Phys. Rev. A* **1981**, *24*, 1520.
- (17) Goulon, J.; Greffe, J.-L.; Oxtoby, D. W. *J. Chem. Phys.* **1979**, *70*, 4741.